Imperial College London

Final Report for MSc Individual Project

Predicting motor intention from EEG for neuroprosthetic applications

Author:
Sofia Lopes Monteiro

Supervisor:
Professor Dario Farina

Submitted in partial fulfillment of the requirements for the award of
MSc in Human Robotics from Imperial College London

September 2017 Word count:

Feedback box for project markers:

What I liked about the report:
What could/should be improved:

Predicting motor intention from EEG for neuroprosthetic applications

Final Report for MSc Individual Project

Sofia Lopes Monteiro

Abstract

Research on non-invasive detection of neural-correlates of movement has recently focused on latency. Earlier reliable decoding of motor commands is essential for proper control of neuroprostheses and biofeedback-based rehabilitation, whose performance is currently limited by late detection. We propose novel spatial filters to enhance early phases of movement related cortical potentials (MRCP), improving accuracy and latency of movement prediction. Filter-coefficient computation is based on signal-to-noise-ratio (SNR) of nine electroencephalogram (EEG) scalp channels, after re-referencing or selecting independent and principal components (IC and PC). From a 15 training events, we obtain templates and extract features to detect subsequent movements, using matched filter (MF) or support-vector-machine (SVM), respectively. Processing and classification methods are compared using three measures of detection performance (DP): true positive rate, false positive rate and mean latency (TPR; FPR; Lat). When combined with common average referencing (CAR), SNR-weighting significantly improves DP relative to controls ($p < 0.05$). IC-based channels further improve selectivity ($p < 0.05$), with average performance $85.05 \pm 5.94\,\%$; $2.70 \pm 0.46\,\mathrm{m}^{-1}$; $-263 \pm 95\,\mathrm{ms}$ with MF, and $73.87 \pm 5.04\,\%$; $2.15 \pm 0.80\,\mathrm{m}^{-1}$; $-272 \pm 92\,\mathrm{ms}$ with SVM. Off-line MRCP detection precedes electromyogram (EMG) detection with statistical significance. Our results suggest that SNR-based channel processing may be improve overall detection performance.

Acknowledgements

1 Introduction

Successful man-machine interfaces rely on neuro-muscular state decoding. Research on brain-machine-interfaces (BMI) has generated technologies that benefit extreme cases of communication (e.g. locked-in patients) and motor impairment. Motor and neuroprosthetics have merged to provide machine-assisted movement control, driven by brain switches. Although implantable systems show encouraging results, enabling control of prosthetic limbs with seven degrees of freedom [1], non-invasive devices are still confined

to slow action and low-dimensional space [2]. BMI extension towards comprehensive and user-friendly applications requires faster and more accurate mental command detection [3].

Surface EMG has been widely employed in prosthetic control and biofeedback-based rehabilitation [4][5]. Electrical muscle signals initiate shortly before movement onset and can be detected with accuracy close to 100 % using simple processing [6][7]. Although reliable and non-invasive, this modality is intrinsically limited in time by the arrival of action potentials to the neuromuscular junction. While EMG is highly accurate, its delayed activity onset cannot fulfill the requirements of complex man-machine interfaces. The subsequent electromechanical delay is variable (e.g. depending on fatigue level [8] or contraction type [9]) and insufficient for enabling human-like machine responses: for instance, isometric knee extension EMG onset may precede motor-output by 20 to 100 ms [10].

EEG is a promising non-invasive alternative for earlier detection of movement intention, as it captures brain activity related to motor commands (i.e. the efferent signals to motor nerves). Consequently, recent studies on EEG have focused not only on accuracy, but also on the earliness of detection with respect to movement onset [11][12].

Movement performance or imagination activate the ipsi- and contralateral regions of the motor cortex that represent the moved or imagined limb [13]. Synchronous brain activity related to motor preparation generates cortical potentials that precede motor tasks and can be detected by scalp electrodes over the cortex [13]. These early neural-correlates of movement intention are possible predictors of movement initiation, and consist in several signals of different nature, including oscillatory (e.g. ERD, event related desynchronization) or a-periodic activity (e.g. MRCP) [14].

The Bereitschaftspotential (BP; i.e. readiness potential) anticipates movement initiation by up to 2 seconds and is observed in EEG after averaging over events to reduce noise [14]. It is the first part of the MRCP: a spontaneous, low-frequency, negative activity peak evoked in both real and imagined movements [14]. The anterior supplementary motor area (SMA) and the pre-SMA have been proposed as the main anatomical origins of BP [15]. Dorsiflexion MRPCs have been described using EMG as reference: a slow

negative phase occurs from 1 s to 100-50 ms before EMG onset (t_0), followed by a short peak and a steeper downward slope ending 50-150 ms after t_0 [16][17]. In the literature, MRCP detection latency is typically reported with respect to movement onset or peak negativity.

In closed-loop applications, fast detection allows control over the timing of afferent signal delivery, which is believed to be essential in neuroplasticity [18]. Using MRCP and following the suggested limits for feedback latency (300 ms [18]), cortical potentiation can be induced in both healthy subjects and stroke patients [19]. In addition to having an early onset and well defined behaviour prior to movement, MRCPs are observed even in subjects with no BCI experience, whereas other neural correlates, including ERD, require intensive practice before subjects can produce detectable signals []. Possible applications of improved MRCP detection include clinical research, prosthetic control, motor rehabilitation, human augmentation or athletic training.

Since MRCPs have low energy against the background EEG signal (e.g. noise, artifacts), signal enhancement with spatial filters (e.g. linear combinations of several channels) is typically done before detection [12]. The literature describes numerous filtering approaches whose output are surrogate channels (SCs), whose time windows are then classified [14].

The simplest spatial filters in EEG processing are not dependent on the data and have fixed coefficients: based only on the electrode grid location, signal re-referencing highlights local activity under scalp channels [20][21], The most conventional techniques are common average referencing (CAR) and large Laplacian filtering (LLF) [14]. The re-referenced apex electrode Cz is applied by many protocols involving dorsiflexion, since the central-medial scalp has been reported to capture higher amplitude BP activity [22][14][12]. The LLF-filtered Cz is used in [23] and [24], while CAR is used in [11].

However, the SNR-based optimal spatial filter OSF performs better than LLF, with high average accuracy ($82.5 \pm 7.8\%$) and ML (-66.6 ± 121) [24], Although movement prediction is negative, it is not statistically significant. OSF also leads to successful MRCP detection with a global, subject independent, template, which performs only

slightly worse than individual templates [25]. These findings sustain the stability of slow potentials – not only across time but across subjects – whereas ERD is irregular across individuals and even different runs of the same subject [26].

Additional popular data-driven transformations in BMI research may contribute to improve MRCP detection, including statistics-based decomposition methods – principal component analysis (PCA), independent component analysis (ICA) or common spatial patterns (CSP) [20]. CSP separates signal components in a supervised way, emphasizing the contrast in variance between different signal portions [20]. However, CSP seems prone to over-fitting in MRCP detection and is outperformed by LLF and OSF [24]. PCA is typically employed in dimensionality reduction, allowing selection of the characteristic directions (i.e. eigenvectors) responsible for the most of the variance among the data and exclusion of the less discriminatory ones [27] – this is especially convenient in the process of feature selection for training classifiers []. While PCA can return decorrelated linear combinations of channels, ICA further separates the signal into statistically independent projections of the signal and isolates signals from different sources. Therefore, ICA is widely used in artifact removal (e.g. extraction of the electrocardiogram ECG or the electrooculogram EOG), being more effective than PCA for that purpose [20]. Despite improving accuracy of MRCP detection [21], current ICA-based methods require visual inspection of the unmixed signal. A more elegant component extraction method employs constrained-ICA (cICA) to detect MRCPs in an off-line study: it finds a *signal-direction* of interest by biasing the analysis toward a reference signal [12] – resulting in good accuracy and negative ML (87.11 ± 11.73, 20.69 ± 13.68, -34 ± 29 ms) [12]. However,it is unpractical to construct a reference signal with the appropriate periodization of signal/no-signal (i.e. MRCP/no-MRCP) for application in on-line self-paced movement detection.

After spatial-filtering, a matched filter (MF) can further enhance the SNR by comparing incoming signals with MRCP templates (averages of training events) []. The MF output reflects the correlation of the input signal with the expected MRCP morphology. Movement detection can then be performed by setting a proper threshold on that signal [].

Alternative classifiers for MRCP include linear discriminant analysis (LDA), support vector machine (SVM) or k-nearest neighbours (k-NN) []. A combination of locality preserving projections (LPP) – another technique for dimensionality reduction – and LDA outperforms MF in MRCP detection, especially under reduced attention levels, suggesting that classifiers may be more powerful in ergonomic conditions [23] [28]. The worse accuracy and latency of MF is attributed in part to training exclusively from signal epochs (i.e. extracting templates) [23], thus wasting any available information about noise (this may also explain why the LLF performs worse than OSF, since the computation of the later is based on SNR). Strict sense classifiers, on the other hand, are trained with both signal and noise epochs [27].

Using time domain features and LDA, [29] correctly classified motor events from MRCP, but the purpose of that study was to distinguish between event types, not between event and no-event phases. Supervised learning is also employed in ERD-based detection [], in which spectral features are widely employed. Analysis of ERD in the frequency domain is informative, as it is related to oscillatory phenomena lasting for relatively long periods. ERD can be detected from power spectral density (PSD) analysis and a Naïve Bayes classifier, after extracting discriminatory frequencies and channels in the training phase [26]. Time frequency analysis of ERD with the wavelet transform has also been used to detect movement intention [30] [20]. When comparing LDA performance with MRCP (using time domain features) against ERD (using frequency domain features), the later led to better DP [31]. In the same study, MF performed worse than LDA based on either spectral or temporal features [31].

This study aims at designing methods to detect movement intention for the benefit of prosthetic and rehabilitative applications. As our target population comprises impaired subjects, the MCRP emerges as an appropriate neural correlate for detection because it is stable, does not require lengthy and potentially frustrating training, and has been successfully detected in stroke patients. In an off line evaluation, we explore novel sets of spatial filters based on SNR and component analyses. Our goal is to improve EEG processing so that accurate movement detection – using either MF or classifiers – can

anticipate the currently most reliable technique, based on EMG. The first hypothesis is that intention of movement can be detected earlier from EEG than with EMG; the null hypothesis is that the average latencies of different detection techniques are not significantly different from zero (i.e. $t_0 = 0$ is the moment of EMG detection),

From the statistical analysis of the first hypothesis, we compare several combinations of processing and classification techniques. We adopt true positive rate (TPR), false positive rate (FPR) and mean latency (ML) as measures of detection performance (DP). To balance them properly, movement prediction and sensitivity (i.e. negative ML and TPR) should not compromise selectivity (i.e. FPR) relative to other currently available techniques.

In an initial heuristic attempt to improve SNR, we compute the SC as a weighted averages of scalp channels, proportionally to their mean SNR. This weighted spatial filter (WSF) is compared to the greedy spatial filter (GSF), which selects only the channel with highest SNR. We also evaluate the effect of re-referencing the scalp channels before determining the WSF/GSF coefficients. ICA and PCA are then introduced to facilitate selection of channel-space directions with enhanced SNR. We assess whether automatic selection of components, based on their mean SNR, leads to good DP, to overcome the need for manual extraction of artifact contaminated components. Re-referencing of the central channel Cz is used as the control filtering method. After the former investigation, hinged on MF-threshold detection, we select the best preforming filters and confirm whether they also lead to improved classification with SVM.

2 Methods

All computational methods were implemented in MATLAB, using the *Signal Processing*, *DSP System*, *Statistics and Machine Learning* and *Wavelet* Toolboxes. Besides the *FastICA* package (see Section 2.3.4), all scripts were independently developed.

2.1 Data Acquisition

This study investigates part of the data acquired in [19], where seven healthy subjects performed self-paced ballistic right ankle dorsiflexion, aided by a visual feedback system to reach force within a target range[1]. EMG and nine EEG channels (F3(FC1), Fz, F4(FC2), C3, Cz, C4, P3(CP1), Pz and P4(CP2)) were sampled at 1200 Hz. Each run of about 30 dorsiflexions was split into training and test sets, which were processed separately. Training data contained 15 events, which has been reported as minimum amount of MRCPs for correct classifier training [28]. The size of training and test data is substantially inferior to the standard in similar works.

2.2 Pre-processing

After removing the linear drift, second order band-pass butterworth filters were applied to all channels (bandwidths 0.05–3 Hz for EEG; 30–250 Hz for EMG). EMG was subtracted from its mean and rectified. Event onsets t_{0i} were detected when the rectified EMG reached 4 times its overall average, which matched the instants identified in [19].

The procedures described in the following sections (e.g. SNR analysis, MF template, labeled training sets for SVM) employ pre-selected epochs containing signal (MRCP) and noise (background activity). Two second long windows were selected from the training signals. The i^{th} signal epoch starts 1.5 s and ends 0.5 s after t_{0i}; the corresponding noise epochs go from 4 s to 2 s before t_{0i} [2]. Noise and signal epochs were used to train SNR-based filters (see Section 2.3) and classifiers. For each spatial filter, the signal epoch average across training events is the subject's individual template.

[1]The full data used in offline analysis and filter validation consisted in one run per subject and correspond to a fraction of the training set used in [19].

[2]The same epoch limits are found throughout the literature []. We compared different windows in a short preliminary study indicating that [-1.5;+0.5] s led to better results than [-1.5;0], [-2;0], [-2;+0.5] or [-2;+1] s.

2.3 Spatial Filtering

2.3.1 SNR Analysis

SNR analysis is used – both directly or indirectly – to determine the coefficients of novel spatial filters (Figure 2.3.1 shows a diagram of the main processing stages).

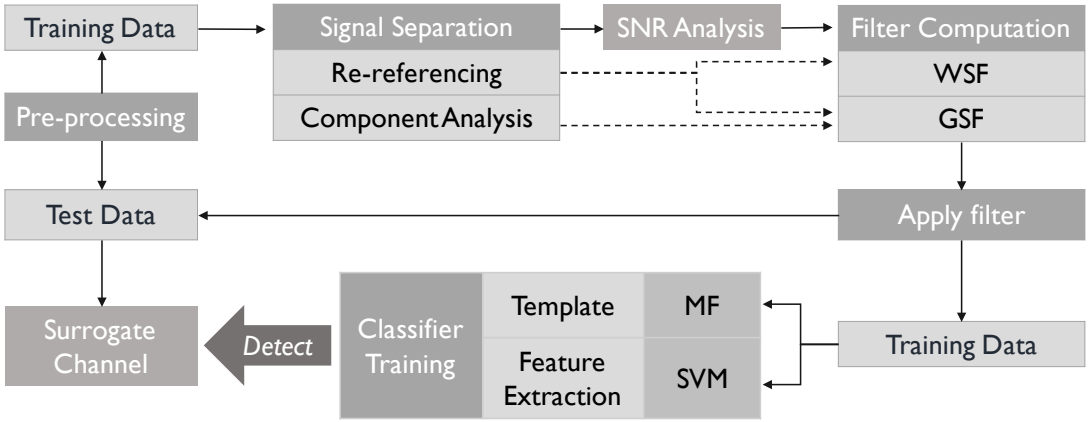

For all channels/components, we determined each event's SNR (i.e. the quotient of the sum of squared magnitudes of signal and noise epochs), before and after processing EEG. The mean SNRs of channels/components across events was used to compute/select spatial filters.

2.3.2 Channel Re-referencing

Pre-filtered scalp channels were processed with large Laplace filter (LLF), subtracting to each channel the mean activity of its orthogonal channels, and common average referencing (CAR), subtracting to each channel the mean activity of all channels. The resulting re-referenced multi-channel signals (LLF-EEG and CAR-EEG) were analyzed as detailed in Section 2.3.3 [20][14].

2.3.3 Weighted and Greedy Spatial Filters

The weights of channels with negative mean SNR were set to zero. The remaining channels are weighted proportionally to their mean SNR and the final coefficients are normalized. The WSF output is the weighted average of channels with positive mean SNR across training events. The GSF selects only the channel with maximal SNR. Both filters were

used to compute surrogate channels from different inputs: pre-processed scalp channels (PRE-EEG), LLF-EEG and CAR-EEG.

2.3.4 Independent and Principal Components

The pre-processed training EEG was analyzed with the *FastICA* and PCA functions of MATLAB, yielding *unmixing* and *decorrelating* matrices, respectively. To obtain independent component (IC) and principal component (PC) templates, training signal epochs were projected into the directions given by the corresponding matrices and averaged across events[3]. The same projections were employed on the test signal to obtain SCs.

In all subjects, visual inspection immediatelly revealed that at least one IC and PC captured the stereotypical MRCP shape (see Figure **??**). With both ICA and PCA, SNR analysis of projected training epochs confirmed that the training components with maximal SNR were MRCP-shaped (see Figure 11d); furthermore, the corresponding templates and spatial filters led to the best DP among all components. These preliminary results inspired a fully automatic filter computation: for each subject, the set of ICA/PCA-based coefficients is the *unmixing*/*decorrelating* vector corresponding to the IC/PC with highest mean SNR in the training data. We note that the proposed methods apply analyses algorithms exclusively in the training phase, avoiding their computational burden (which is considerably high for ICA) while testing. This is essential for an eventual on-line implementation.

2.4 Estimation

2.4.1 Matched Filter & Threshold

The MF is implemented by convolving the template with the input signal. Each spatial filter is applied to the test EEG leading to a SC which is the input to the MF. The impulse response is the time reversed template of the corresponding spatial filter. Estimation as MRCP/non-MRCP is done by setting a threshold for the MF output.

[3]The number of PCs is equal to the number of channels, while ICs may be less or equal.

An initial study employing different thresholds to each MF output revealed a clustered distribution of the three-dimensional DP, in which each spatial filter generated a ROC "cluster". The mean performance across a small threshold range may thus reflect the **relative** performance of a spatial filter. Withing each ROC, the behaviour of DP measures followed the expectations: higher thresholds worsened latency and decreased both TPR and FPR, and vice versa. Instead of fine tuning thresholds for each filter and subject, several thresholds were applied in a well defined and automatically generated range that was independent from the type of filter.

2.4.2 Linear Classifiers

A simplified selection of time domain features was inspired by [29]. Due to the different nature of this study (see Section 1), we altered some features to increase robustness against noise, finally selecting the following: 1) maximum absolute amplitude, 2) wavelength, slope of linear regression from: 3) beginning to peak, 4) peak to end, 5) beginning to 50 ms before peak.

Different spatial filters were applied, and acceptable DP was achieved only with ICA (e.g. LLF-Cz resulted in no selectivity). In the initial stage of feature selection, both SVM and LDA were investigated. As the later was consistently less selective and only slightly more sensitive, we report the results obtained with SVM.

SVM is trained with features obtained from signal and noise training epochs, after filtering with ICA (i.e. the maximal SNR IC). Testing at each instant was done by classifying the previous 2 second long segments of filtered input data at every 10 ms interval.

2.5 Statistical Analysis

One way tests were used to compare the DP of spatial filters processed with MF: ICA, PCA, CAR-GSF, CAR-Cz and LLF-Cz. All measures were tested with the non-parametric Kruskal-Wallis test; one way ANOVA was also performed on ML, to test hypothesis 1. The average MF DP of the best filter was compared with the best performing SVM, using the Kruskal-Wallis test. In the case of significant differences, multiple comparisons with

Bonferroni correction tested pairwise differences, with significance level $p < 0.05$.

3 Results

Table 1 shows the mean performances of the best performing SNR-weighted filter, PCA, ICA and controls. Detailed subject performance is in Appendix (). Overall, the proposed filters based on ICA, PCA and CAR-SNR (CAR-WSF and CAR-GSF) were significantly more accurate.

The Kruskal-Wallis test resulted in significant differences among the means of all performance measures ($p = 0$). Multiple comparisons ($p = 0.05$) showed that ICA, PCA, CAR-WSF and CAR-GSF had significantly higher TPR than control filters (CAR-Cz and LLF-Cz). ICA had significantly lower FPR than CAR-Cz and all LLF-based filters. PCA had FPR significantly lower than LLF-WSF and controls. Controls had significantly higher FPR than all filters apart from LLF-WSF. ICA had significantly larger (i.e. more negative) latency than CAR-Cz. CAR-WSF and CAR-GSF had significantly larger latency than both PCA and CAR-Cz. One-way ANOVA yielded the same significant differences as the Kruskal-Wallis test for ML of spatial filters ($p = 0$). Moreover, it revealed that the confidence intervals for ML averages were entirely negative, except in the case of PCA and CAR-Cz filtering, confirming hypothesis one.

Table 1: Average True Positive Rate, False Positive Rate and Mean Latency for offline movement execution detection.

Method	TPR %	FPR $/min$	ML s
LLF-Cz-MF	55.32 ± 10.97	6.56 ± 0.70	-239 ± 133
CAR-Cz-MF	63.92 ± 10.11	6.51 ± 0.75	-31 ± 187
CAR-GSF-MF	89.29 ± 3.17	3.79 ± 0.32	-379 ± 87
PCA-MF	82.85 ± 7.00	3.38 ± 0.30	-107 ± 70
ICA-MF	85.05 ± 5.94	2.70 ± 0.46	-263 ± 95
ICA-SVM	73.87 ± 5.04	2.15 ± 0.80	-272 ± 92

All methods apart from SVM were processed with a matched filter and threshold. For each method results were averaged across subjects (average $\pm$ standard error)

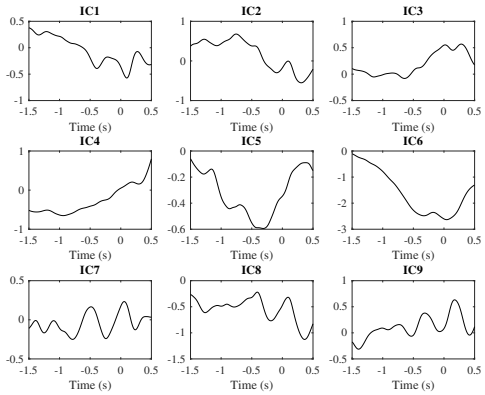

(a) ICA templates

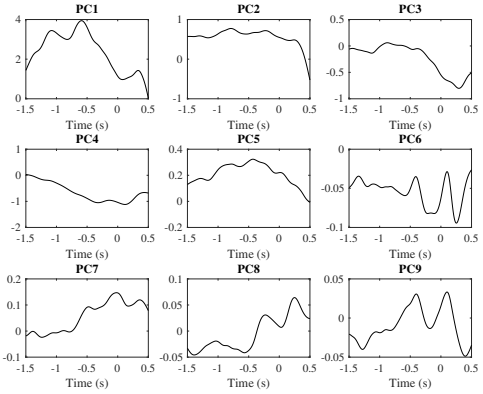

(b) PCA templates

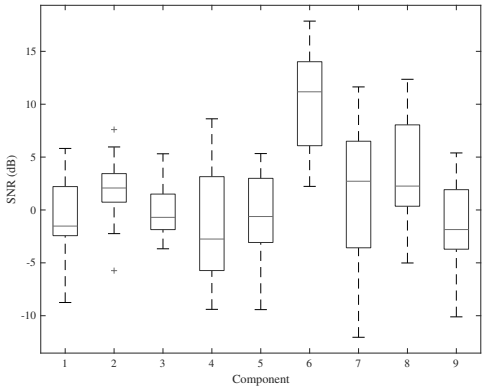

(c) SNR of independent components

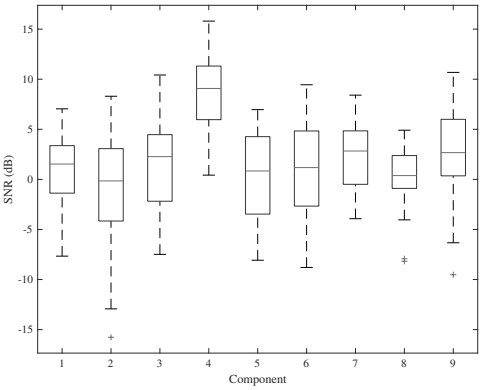

(d) SNR of principal components

Figure 1: (a) and (b) are templates (average of training events) of independent and principal components; (c) and (d) SNR of independent and principal components (distribution across epochs) [Subject 5].

4 Discussion

4.1 Improving Movement Prediction

4.1.1 Greedy Spatial Filter

Weighting channels proportionally to their own SNR seems to improve DP substantially. However, results are significantly dependent on the type of local signal enhancement employed. SNR-weighted methods alone (i.e. without re-referencing) did not achieve the desired DP (FPR $> 10\,\mathrm{m}^{-1}$); if combined with LLF, they did not outperform control filters significantly in any parameter. However, when preceded by CAR, they improved overall DP: both CAR-WSF and CAR-GSF outperformed all other filters in TPR and ML, without significantly increasing FPR relative to the best results (ICA and PCA), while significantly improving accuracy (TPR and FPR) relative to controls. This method's

Table 2

	ICA			PCA			CAR-Cz		
	TPR %	FPR /min	Lat s	TPR %	FPR /min	Lat s	TPR %	FPR /min	Lat s
Subject 2	88.0	3.44	-281	86.5	4.18	-124	62.0	5.88	82
Subject 3	73.9	3.06	149	54.0	3.48	175	23.3	7.29	1118
Subject 4	100.0	1.52	-556	94.1	2.78	-216	64.0	3.27	334
Subject 5	98.1	1.28	-260	95.6	2.60	-347	16.2	5.93	-771
Subject 6	70.6	2.68	-441	95.0	3.00	-56	100.0	3.79	139
Subject 7	57.1	7.24	65	61.4	4.57	98	59.8	6.81	314
Mean	81.3	3.2	-221	81.1	3.4	-79	54.2	5.5	202

Average detection performance using a matched filter and channel combinations based on 1) independent component with maximal SNR - ICA; 2) principal component with maximal SNR - PCA; 3) CAR-Cz.

Table 3

	CAR-GSF			CAR-Cz			LLF-Cz		
	TPR %	FPR /min	Lat s	TPR %	FPR /min	Lat s	TPR %	FPR /min	Lat s
Subject 2	81.0	3.43	-392	62.0	5.88	82	53.5	6.99	35
Subject 3	81.2	2.68	-69	23.3	7.29	1118	22.7	6.10	-506
Subject 4	100.0	1.88	-602	64.0	3.27	334	37.5	3.48	336
Subject 5	82.5	3.20	-301	16.2	5.93	-771	13.1	5.28	-155
Subject 6	100.0	3.18	-234	100.0	3.79	139	99.4	4.10	106
Subject 7	82.1	4.17	72	59.8	6.81	314	53.8	7.24	351
Mean	87.8	3.1	-254	54.2	5.5	202	46.6	5.5	27

Average detection performance using a matched filter and channel combinations based on 1) CAR-GSF; 2) CAR-Cz; 3) LLF-Cz.

performance may be appropriate in applications without stringent requirements on selectivity (e.g. neuro-rehabilitation), providing earlier detection with high sensitivity.

The somatotopic organization of many cortical areas, including the SMA [32] ensures an univocal correspondence between the spatial sources of brain activity and the resulting actuated muscles. Thus, for a given movement, the adequate placement of scalp electrodes for capturing activity can be roughly predicted. However, as SNR analysis shows (see Figure **??**), the channels with maximal MRCP-SNR vary among subjects. Also, the Cz channel placed in the central-medial scalp had a much lower SNR than any weighted surrogate channel. This is consistent with the good performance of OSF and the more naïve WSF and GSF over the anatomically based Cz channel. Coefficient adjustment based on channel properties may be extended to a more supervised adaptive on-line

method that updates the channel weights as new events are observed; this may further reduce the impact of experimental conditions (e.g. electrode displacement) or subject variability.

The weighted combination of filters (WSF) has practically the same results as the channel with highest SNR alone (GSF). After removing common activity, the single channel with maximal SNR provides enough information for successful detection, and other channels seem to have residual impact – GSF seems preferable to WSF, as it avoids have unnecessary complexity. In fact, the relative "strength" of BP over the scalp changes throughout the MRCP, initially being more pronounced around the central-medial scalp and moving towards the primary motor cortex closer to movement onset [33][14]. This suggests that combined channel information could have a higher MRCP signal content than any channel alone. Although in this study the weighted-average does not outperform a single channel, a more refined estimation method adjusting coefficients depending on the phase of the MRCP could have better results.

4.1.2 Component Analysis

Both ICA and PCA resulted in significant improvement in selectivity (FPR) and sensitivity (TPR) from controls, demonstrating that a single component selected on an SNR basis can capture enough information for accurate MRCP detection. ICA allows prediction of movement, whereas PCA's ML confidence interval still includes positive values. Furthermore, ICA-MF trended towards lower FRP than all other filters and ICA-SVM resulted in even smaller FRP (while other filters led to no selectivity along with SVM). Although ICA-SVM decreased the mean TPR in about 11% relative to ICA-MF, this difference was not significant; mean ML was slightly decreased, remaining in a fully negative confidence interval.

Although the best trade-off between reliability and prediction of movement was achieved with ICA-based spatial-filtering, we note that the computational burden of ICA training with respect to PCA and SNR-weighted filters is extremely high. While this impacts only the training phase, our study detects MRCPs using information obtained in the same run

where we test: we have not assessed the possibility of component selection based on analysis of different runs, and therefore have only ground for suggesting an adaptive on-line training approach. To access the usefulness of these methods in real-time, further work should be done to estimate how many training events are necessary in order to decompose the signal and select the useful components.

This automatic method projects the input signal into a principal direction (i.e. IC/PC with maximal SNR in the training set is a reference frames) before predicting movement with a MF-detector or SVM. With PCA, we attempt to select a channel combination that captures the MRCP and is not correlated with other signal components. ICA *unmixes* scalp signals into statistically independent components, further eliminating higher order dependencies: it attempts to separate activity of different signal sources, which may be related to its better DP.

In all subjects, there is a single independent component (for both ICA and PCA) with significantly higher SNR than the remaining ones (even when the algorithm does not extract as many sources as the number of scalp channels, which may happen in ICA). The template generated from this component captures the MRCP morphology, and leads to the best detection results among all components. We note, however, that the component with maximal SNR is not necessarily the one in which the data has maximal variance (i.e. first eigenvector). Despite the likely loss of MRCP related information by selecting a single component, detection is always improved relative to our baseline value and seems promising when compared to methods presented in the literature. This may be due to the effective attenuation of noise and artifacts, which is evident by visual inspection of the components with maximal SNR.

4.1.3 Linear Classifiers

Previous works comparing MF to LDA were based on LLF-Cz, which had been shown to yield sub-optimal results with MF [24][28][23]. In this method, information about noise was not considered when implementing the MF (obtaining SC and templates). Our results compare DP of MF and SVM – another linear classifier – only after applying

a spatial-filter chosen from SNR-analysis. When pre-filtering with ICA, there was no statistical difference between detection measures from MF and SVM.

The data used in our offline analysis correspond to part of the training set of a study which applied LPP-LDA and reported lower TPR ($73 \pm 10.3\%$) and FPR ($1{,}3 \pm 0.5$/min) [19](see Section 1). We used the indicated minimum number of trials for classifier training (see Section 2.4.2). Avoiding artifact-extraction may have led to less robust templates, contributing to the our worse FPR.

Using LDA trained with the early phase of the MRCP (early BP), [11] achieved high TPR ($76 \pm 7\%$) with a promising average latency of -460 $\pm$ 85 ms in an offline implementation (ML with respect to movement onset). However, a quantitative measure of FPR was not reported. We applied a similar methodology in a preliminary study, where training-epochs were downsampled to 4 Hz and used as feature vectors for LDA and SVM classification. Both resulted in selectivity below chance level. Which was possibly due to unsuficient training data.

4.1.4 Reference Parameters

Different measures of FPR are applied throughout the literature, and usually it is not clear how they are implemented. However, it seems evident that our baseline filters performed worse than in studies [24].

Instead of using *non-rereferenced* channels as baseline, we evaluate the results of the novel spatial filters against the standard re-referenced Cz, which are stronger controls. With MF, control-filters achieved acceptable DP, although with lower accuracy (lower TPR and higher FPR) than the best found in the literature, which may be due to the small number of training epochs []. With SVM, controls led to no selectivity. We reiterate that the current study applies a particular training scheme based on initial events, and uses it to detect the immediately following events (i.e. in the same run). This may be a limitation as we do not evaluate whether training and testing in different runs (due to lack of data). At the same time, it shows the potential for fast on-line training.

We define event onset t_0 as the moment of electrical muscle activity detection, which

precedes movement initiation. This choice of time reference favors our ML measurements when comparing with similar works. We do not however, attempt to quantify that difference, as the electro-mechanical lag is highly variable (see Section 1).

4.2 Preprocessing

4.2.1 Accuracy vs. Latency Trade-Off

Detectors were trained with signal epochs containing a significant portion, but not the entire MRCP [23]. While including the 0.5 s segment after t_0 compromises ML, this strengthens the template matching potential [12], balancing accuracy and early detection [23]. A short evaluation of the impact of shortening the template to [- 1.5, 0 s] slightly improved ML and decreased accuracy with MF, but not with SVM. Our choice of features make SVM more robust to the window choice than the MF – detecting MRCPs before EMG as long as the analyzed segment includes the MRCP peak.

4.2.2 Artifact Corruption

The above results focus on a time domain analysis of the signal but rely on preliminary selection of adequate frequencies. To minimize pre-processing, band-stop or notch-filters (e.g. 50 Hz notch filter for the EMG signal) are not employed. We also avoid visually identifying and extracting artifact-containing epochs in the training phase, ensuring fully automatic training and processing. Although some epochs were corrupted by 1 Hz artifacts with higher amplitude than MRCPs, those were averaged-out in the templates, which revealed the expected MRCP morphology. In such cases, artifacts may still adversely influence DP, as we do not ensure that SCs are not contaminated. Artifact contaminated templates may not only reduce the likelyhood of matching with a real MRCP (therefore reducing the TPR), but may also increase the chance of matching other artifacts in the absence of MRCP (increasing the FPR). This is an essential difference relative to protocols from similar work reported in the literature, which may explain the higher FPR rates in the current study. Offline ERD-based detection without artifact removal allows early detection of movement with high sensitivity, but considerably worse selectivity [26].

The EEG bandwidth 0.05-3 Hz excludes un-informative activity and preserves most signal frequencies from which the MRCP is identified. However, wavelet analysis performed on the 0.05-3 Hz bandwidth seemed to indicate that the most relevant time-frequency phenomena occured in the lower frequencies. Once the methods had been developed, we tested them using the 0.05-1 Hz bandwidth, with no striking changes in overall performance. Good performance in such narrow frequency-band may result from it containing the gross of MRCP – according to wavelet analysis – or to the elimination of artifact containing frequencies.

4.3 Limitations

The methods here presented are trained and tested in different executions, but these are done in the same run. From the current study, it is not possible to infer whether an estimator will perform well in different runs, and these methods should be validated in different runs of the same subject. Our findings support the possibility of training a classifier with a short number of consecutive motor events and correctly predicting subsequent events (in the same run). This may be further explored in on-line adaptive detection.

Also, the training and testing sets were split by choosing a training set with a fixed length. In a few cases this lead to separation of event EMG and EEG detectable activity at the ends, which could be further distorted by filter artifacts. A warning was displayed in the command window every time the run splitting was such that it occurred within 0.5 s of an event, and in that case the last event epoch was not included in the training set. This practically resulted in wasting events, and could have been avoided by separating the data by number of events rater than periods. Apart from not benefiting from the discarded event (this type of studies usually uses many more events for training [19]), the templates were not morphologically affected. However, there could have been residual unmatched EMG (or even EEG) detectable activity at the beginning of the training set. This limitation may have contributed for decreasing TPR (or increasing FPR), especially in the case of classifiers.

Our data corresponds to single-joint movements performed with biofeedback assistance so that force remains within a certain range. Research on MRCP detection during gait initiation has yield reasonable TPR, but with poor FPR and long latency [28]. We may thus anticipate considerably lower performance in compound movements requiring multiple limb and joint motor control, or performed without bio-feedback (i.e. in ergonomic conditions).

5 Conclusion

In an off-line method exploration, we showed that movement execution can be predicted with significant anticipation relative to EMG detection. This can be achieved either with a signal-processing method – MF combined with ICA or SNR-weighted filters – or with a machine-learning approach – SVM if combined with ICA. We reinforce the relevance of MRCP as a strong non-invasive neural-correlate of movement, whose morphology alone provides enough features for prediction. Spatial filters are trained from a limited amount of training events (i.e. up to 15) and enable detection of the following movement executions within the same trial. We show that relevant signal projections can be automatically selected in the training phase, leading to improved DP. The proposed methods can be implemented on-line with reduced computational complexity. Real-time detection of MRCP has the potential for driving closed-loop feedback systems with a latency close to physiological levels. This may allow natural control of neuroprostheses or delivery of properly timed neuro-feedback signals, promoting neuroplasticity and neuromechanical performance (e.g. for stroke rehabilitation or athletic training).

References

[1] J. L. Collinger, B. Wodlinger, J. E. Downey, W. Wang, E. C. Tyler-Kabara, D. J. Weber, A. J. C. Mcmorland, M. Velliste, M. L. Boninger, and A. B. Schwartz, "High-performance neuroprosthetic control by an individual with tetraplegia," *Lancet (London, England)*, vol. 381, February 2013.

[2] B. Xia, O. Maysam, S. Veser, L. Cao, J. Li, J. Jia, H. Xie, and N. Birbaumer, "Acombination strategy based brain–computer interface for two-dimensional movement control," *Journal of Neural Engineering*, vol. 12, August 2015.

[3] F. R. Willett, A. J. Suminski, A. H. Fagg, and N. G. Hatsopoulos, "Improving brain–machine interface performance by decoding intended future movements," *Journal of Neural Engineering*, vol. 10, April 2013.

[4] C. Ishii, A. Harada, T. Nakakuki, and H. Hashimoto, "Control of myoelectric prosthetic hand based on surface emg," pp. 761–766, IEEE Publishing, August 2011.

[5] D. Hofmann, N. Jiang, I. Vujaklija, and D. Farina, "Bayesian filtering of surface emg for accurate simultaneous and proportional prosthetic control.," 2017.

[6] M. B. I. Raez, M. S. Hussain, and F. Mohd-Yasin, "Techniques of emg signal analysis: detection, processing, classification and applications," *Biological procedures online*, vol. 8, no. 1, 2006.

[7] S. Solnik, P. Rider, K. Steinweg, P. DeVita, and T. Hortobágyi, "Teager–kaiser energy operator signal conditioning improves emg onset detection," *European Journal of Applied Physiology*, vol. 110, pp. 489–498, Oct 2010.

[8] E. Conchola, "The effects of two different intermittent fatigue protocols of the leg extensors and flexors between men and women on electromechanical delay, peak torque, and rapid force characteristics," January 2014.

[9] P. Cavanagh and P. Komi, "Electromechanical delay in human skeletal muscle under concentric and eccentric contractions," *European Journal of Applied Physiology and Occupational Physiology*, vol. 42, pp. 159–163, November 1979.

[10] S. Zhou, M. McKenna, D. Lawson, W. Morrison, and I. Fairweather, "Effects of fatigue and sprint training on electromechanical delay of knee extensor muscles," *European Journal of Applied Physiology and Occupational Physiology*, vol. 72, pp. 410–416, March 1996.

[11] E. Lew, R. Chavarriaga, S. Silvoni, and J. d. R. Millán, "Detection of self-paced reaching movement intention from eeg signals," *Frontiers in Neuroengineering*, vol. 5, July 2012.

[12] F. Karimi, J. Kofman, N. Mrachacz-Kersting, D. Farina, and N. Jiang, "Detection of movement related cortical potentials from eeg using constrained ica for brain-computer interface applications," 2017.

[13] M. F. Bear, *Neuroscience : exploring the brain*. Philadelphia: Wolters Kluwer, fourth edition, international edition. ed., 2016.

[14] A. Shakeel, M. S. Navid, M. N. Anwar, S. Mazhar, M. Jochumsen, and I. K. Niazi, "A review of techniques for detection of movement intention using movement-related cortical potentials," *Computational and Mathematical Methods in Medicine*, vol. 2015, 2015.

[15] J. G. Colebatch, "Bereitschaftspotential and movement-related potentials: Origin, significance, and application in disorders of human movement," *Movement Disorders*, vol. 22, pp. 601–610, April 2007.

[16] C. Shagass, *Characteristics of Event- Related Potentials*, pp. 49–86. Boston, MA: Springer US, 1972.

[17] L. Gilden, H. Vaughan, and L. Costa, "Summated human eeg potentials with voluntary movement," *Electroencephalography and Clinical Neurophysiology*, vol. 20, no. 5, pp. 433–438, 1966.

[18] I. K. Niazi, N. Mrachacz-Kersting, N. Jiang, K. Dremstrup, and D. Farina, "Peripheral electrical stimulation triggered by self-paced detection of motor intention enhances motor evoked potentials," *IEEE transactions on neural systems and rehabilitation engineering : a publication of the IEEE Engineering in Medicine and Biology Society*, vol. 20, July 2012.

[19] R. Xu, N. Jiang, N. Mrachacz-Kersting, C. Lin, G. A. Prieto, J. C. Moreno, J. L. Pons, K. Dremstrup, and D. Farina, "A closed-loop brain-computer interface triggering an active ankle-foot orthosis for inducing cortical neural plasticity," *IEEE Transactions on Biomedical Engineering*, vol. 61, pp. 2092–2101, July 2014.

[20] R. P. N. Rao, *Brain-Computer Interfacing: An Introduction*. Cambridge University Press, Sep 2013.

[21] N. Jiang, L. Gizzi, N. Mrachacz-Kersting, K. Dremstrup, and D. Farina, "A brain-computer interface for single-trial detection of gait initiation from movement related cortical potentials," *Clinical Neurophysiology*, vol. 126, pp. 154–159, January 2015.

[22] H. Shibasaki, G. Barrett, E. Halliday, and A. Halliday, "Components of the movement-related cortical potential and their scalp topography," *Electroencephalography and Clinical Neurophysiology*, vol. 49, no. 3, pp. 213–226, 1980.

[23] N. Ren Xu, K. Ning Jiang, D. Chuang Lin, D. Mrachacz-Kersting, D. Dremstrup, and D. Farina, "Enhanced low-latency detection of motor intention from eeg for closed-loop brain-computer interface applications," *Biomedical Engineering, IEEE Transactions on*, vol. 61, pp. 288–296, February 2014.

[24] I. K. Niazi, N. Jiang, O. Tiberghien, J. F. Nielsen, K. Dremstrup, and D. Farina, "Detection of movement intention from single-trial movement-related cortical potentials," *Journal of Neural Engineering*, vol. 8, no. 6, p. 066009, 2011.

[25] I. K. Niazi, N. Jiang, M. Jochumsen, J. F. Nielsen, K. Dremstrup, and D. Farina, "Detection of movement-related cortical potentials based on subject-independent training," *Medical & Biological Engineering & Computing*, vol. 51, no. 5, pp. 507–512, 2013.

[26] J. Ibáñez, J. I. Serrano, M. D. del Castillo, L. Barrios, J. Á. Gallego, and E. Rocon, *An EEG-Based Design for the Online Detection of Movement Intention*, pp. 370–377. Berlin, Heidelberg: Springer Berlin Heidelberg, 2011.

[27] C. M. Bishop, *Pattern recognition and machine learning*. Information science and statistics, New York: Springer, 2006.

[28] S. Aliakbaryhosseinabadi, N. Jiang, L. Petrini, D. Farina, K. Dremstrup, and N. Mrachacz-Kersting, "Robustness of movement detection techniques from motor execution: Single trial movement related cortical potential," pp. 13–16, IEEE, April 2015.

[29] M. Jochumsen, I. K. Niazi, N. Mrachacz-Kersting, D. Farina, and K. Dremstrup, "Detection and classification of movement-related cortical potentials associated with task force and speed," *Journal of Neural Engineering*, vol. 10, October 2013.

[30] A. Chamanzar, A. Malekmohammadi, M. Bahrani, and M. Shabany, "Accurate single-trial detection of movement intention made possible using adaptive wavelet transform," vol. 2015, 2015.

[31] E. N. Kamavuako, M. Jochumsen, I. K. Niazi, and K. Dremstrup, "Comparison of features for movement prediction from single-trial movement-related cortical potentials in healthy subjects and stroke patients," *Computational Intelligence and Neuroscience*, vol. 2015, 2015.

[32] D. Arienzo, C. Babiloni, A. Ferretti, M. Caulo, C. Del Gratta, A. Tartaro, P. Rossini, and G. Romani, "Somatotopy of anterior cingulate cortex (acc) and supplementary motor area (sma) for electric stimulation of the median and tibial nerves: An fmri study," *NeuroImage*, vol. 33, pp. 700–705, November 2006.

[33] H. Shibasaki and M. Hallett, "What is the bereitschaftspotential?," *Clinical Neurophysiology*, vol. 117, no. 11, pp. 2341–2356, 2006.

Table 4

	GSF			MaxCh			Cz		
	TPR %	FPR /min	Lat s	TPR %	FPR /min	Lat s	TPR %	FPR /min	Lat s
Subject 2	45.0	18.53	265	40.0	19.45	284	52.5	15.74	296
Subject 3	43.2	4.28	92	55.1	3.80	60	36.4	3.43	-74
Subject 4	78.7	12.67	-806	82.4	11.36	-904	65.4	13.27	-865
Subject 5	74.4	12.71	694	55.6	12.74	402	55.6	12.74	402
Subject 6	35.0	18.12	-210	76.9	11.18	-759	76.9	11.18	-759
Subject 7	38.0	10.11	-64	46.2	10.09	-88	31.0	9.86	29
Mean	-	-	-	-	-	-	-	-	-

Average detection performance using a matched filter and channel combinations based on: 1) SNR based channel weighting - GSF; 2) channel with maximal SNR - MaxCh; 3) center electrode - Cz; 4) un-weighted channel average - UW.

Table 5

	CAR/GSF			CAR/MaxCh			CAR-Cz		
	TPR %	FPR /min	Lat s	TPR %	FPR /min	Lat s	TPR %	FPR /min	Lat s
Subject 2	78.5	3.40	-399	81.0	3.43	-392	62.0	5.88	82
Subject 3	81.2	2.74	-64	81.2	2.68	-69	23.3	7.29	1118
Subject 4	100.0	2.14	-541	100.0	1.88	-602	64.0	3.27	334
Subject 5	82.5	3.25	-305	82.5	3.20	-301	16.2	5.93	-771
Subject 6	93.8	2.95	-338	100.0	3.18	-234	100.0	3.79	139
Subject 7	83.7	4.10	68	82.1	4.17	72	59.8	6.81	314
Mean	-	-	-	-	-	-	-	-	-

Average detection performance using a matched filter and channel combinations based on common average reference filtering plus: 1) SNR based channel weighting - CAR+GSF; 2) channel with maximal SNR - CAR+MaxCh; 3) center relectrode - CAR+Cz; 4) un-weighted channel average - UW.

Table 6

	LLF/GSF			LLF/MaxCh			LLF-Cz		
	TPR %	FPR /min	Lat s	TPR %	FPR /min	Lat s	TPR %	FPR /min	Lat s
Subject 2	81.0	4.43	-205	73.0	4.88	-274	53.5	6.99	35
Subject 3	59.7	3.98	-23	34.7	3.98	-225	22.7	6.10	-506
Subject 4	100.0	2.91	-264	100.0	2.70	-302	37.5	3.48	336
Subject 5	54.4	3.45	-335	56.2	2.15	-45	13.1	5.28	-155
Subject 6	78.8	3.84	52	95.6	3.39	181	99.4	4.10	106
Subject 7	67.9	4.15	203	70.7	4.50	153	53.8	7.24	351
Mean	-	-	-	-	-	-	-	-	-

Average detection performance using a matched filter and channel combinations based on large laplace filtering plus: 1) SNR based channel weighting - LLF+GSF; 2) channel with maximal SNR - LLF+MaxCh; 3) center electrode - LLF+Cz; 4) un-weighted channel average - UW.

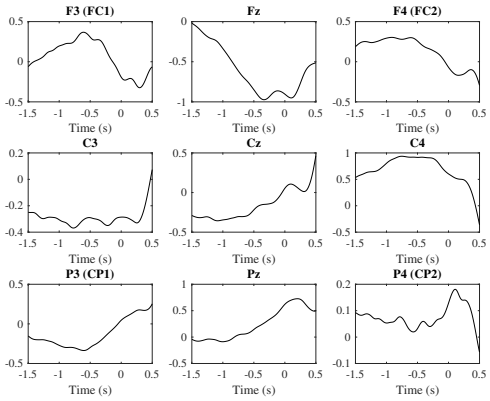

(a) Average of CAR filtered epochs

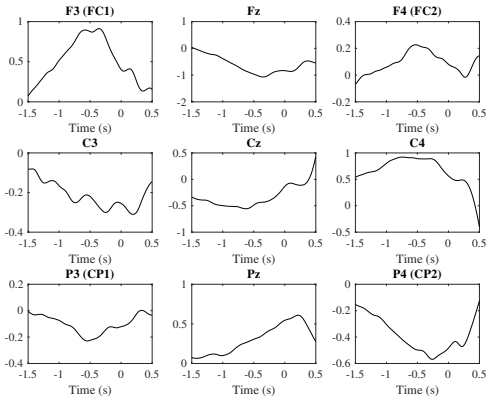

(b) Average of LLF filtered epochs

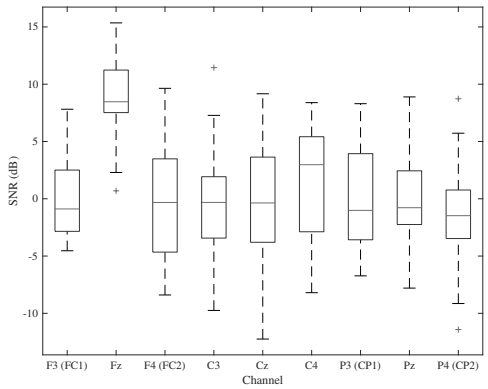

(c) CAR filtered channels SNR

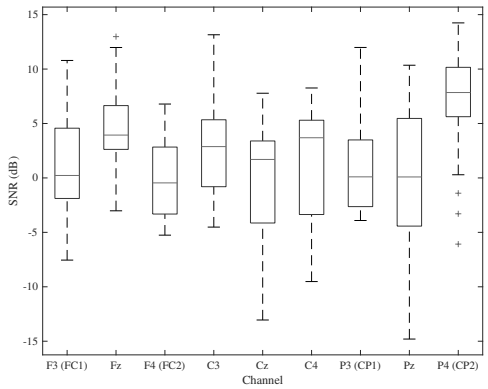

(d) LLF filtered channels SNR

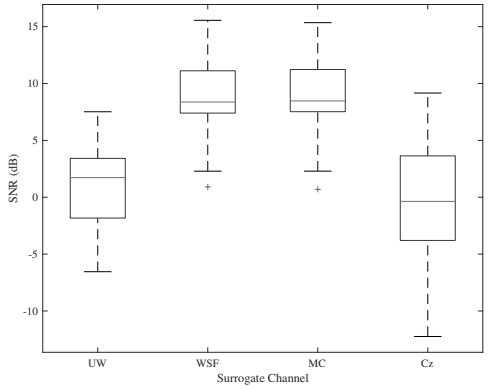

(e) CAR: input SNR vs. GSF output SNR

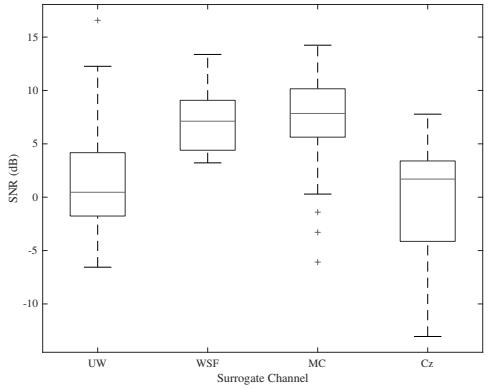

(f) LLF: input SNR vs. GSF output SNR

Figure 2: Channels filtered with CAR and LLF: (a) and (b) average of signal epochs; (c) and (d) channel SNR; (e) and (f) For each epoch, the SNR of the GSF output is a function of the maximal SNR among all CAR (LLF) channels [Subject 5].

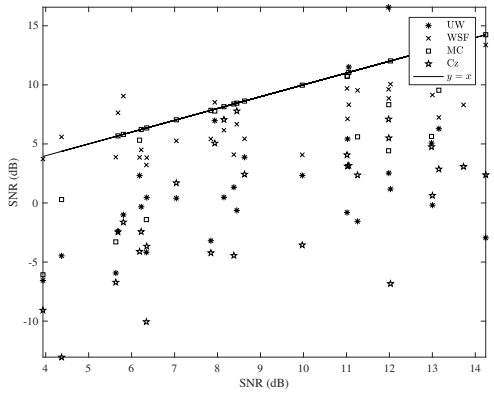

(a) LLF: input SNR vs. GSF output SNR

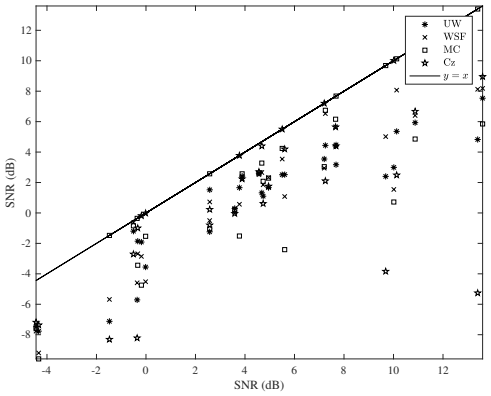

(b) Unfiltered EEG: input SNR vs. GSF output SNR

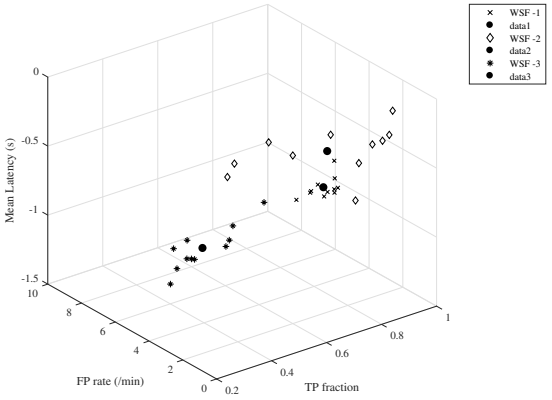

(c) LLF

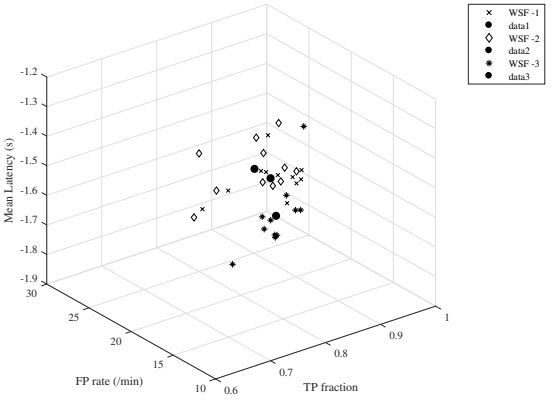

(d) Unfiltered EEG

Figure 3: EEG filtered with LLF and unfiltered EEG: (a) and (b) For each epoch, the SNR of the GSF output is a function of the maximal SNR among all LLF (unfiltered) channels; (c) and (d) Detection performance calculated as TPR/FPR/Lat in a range of thresholds for GSF, the channel with highest SNR and Cz [Subject 5].